Journal of Applied Fluid Mechanics, Vol. 9, No. 3, pp. 1115-1122, 2016.
Available online at www.jafmonline.net, ISSN 1735-3572, EISSN 1735-3645.
DOI: 10.18869/acadpub.jafm.68.228.24584

Casson Fluid Flow near the Stagnation Point over a Stretching Sheet with Variable Thickness and Radiation

G. K. Ramesh[1,2†], B. C. Prasannakumara[3], B. J.Gireesha[2] and M. M. Rashidi[4]

[1]Department of Mathematics, S.E.A College of Engineering and Technology, K. R. Puram, Bangalore, Karnataka, India
[2]Department of Studies in Mathematics, Kuvempu University, Shankaraghatta, Shimoga, Karnataka, India.
[3]Department of Mathematics, Government First Grade College, Koppa, Karnataka, India.
[4]Mechanical Engineering Department, Engineering Faculty of Bu-Ali Sina University, Hamedan, Iran.

†*Corresponding Author Email: gkrmaths@gmail.com*

(Received January 22, 2015; accepted June 29, 2015)

ABSTRACT

The stagnation-point flow of an incompressible non-Newtonian fluid over a non-isothermal stretching sheet is investigated. Mathematical analysis is presented for a Casson fluid by taking into the account of variable thickness and thermal radiation. The coupled partial differential equations governing the flow and heat transfer are transformed into non-linear coupled ordinary differential equations by a similarity transformation. The transformed equations are then solved numerically by Runge-Kutta-Fehlberg method along with shooting technique. The effects of pertinent parameters such as the Casson fluid parameter, wall thickness parameter, velocity power index, velocity ratio parameter, Prandtl number and radiation parameter have been discussed. Comparison of the present results with known numerical results is shown and a good agreement is observed.

Keywords: Stagnation point flow; Casson fluid; Variable thickness; Thermal radiation; Numerical solution.

NOMENCLATURE

A	parameter related with sheet profile
b	parameter related with stretched surfaces
c_p	specific heat
k	thermal conductivity
k^*	mean absorption co-efficient
m	velocity power index
Nr	radiation parameter
Pr	Prandtl number
q_r	radiation heat flux
T	temperature of the fluid
T_0	characteristic temperature
T_w	temperature at the wall
T_∞	large distance from the wall
U	free stream velocity
U_w	stretching sheet velocity
u , v	velocity components of the fluid along x and y directions
x	coordinate along the stretching sheet
y	distance normal to the stretching sheet
μ	coefficient of viscosity of the fluid
ρ	density of the fluid
σ^*	Stefan-Boltzman constant
η	similarity variable
ψ	stream function
α	wall thickness parameter
β	Casson parameter
μ_b	plastic dynamic viscosity of the non Newtonian fluid
π	product of the component of deformation rate with itself
π_c	critical value
λ	ratio of rates of velocities
ν	kinematic viscosity

1. INTRODUCTION

There is an increasing application of non-Newtonian fluids specifically in the flow of nuclear fuel slurries, flow of liquid metal and flow of alloys, flow of plasma, flow of mercury amalgams, and flow of lubrication with heavy oil and greases, coating of papers, polymer extrusion and several others. With such facts in mind, the knowledge of non-Newtonian fluid dynamics with or without heat transfer is quite essential for better understanding regarding food freezing and polymer injection etc. Usually the study of non-Newtonian fluid is much more difficult, because of their complex nature and complex interactions with the flow field. The majority of the information on non-Newtonian fluids is very empirical. The governing equations for non-Newtonian fluid flows are highly nonlinear. Also, the industrial applications of non-Newtonian fluid flow are increasing day by day. Among the many industrial non-Newtonian fluids some fluids behave like elastic solids, and for those fluids, a yield shear stress exists in the constitutive equations. Casson fluid is one of such non-Newtonian fluids. So if the shear stress magnitude is greater than yield shear stress, then flow occurs. Casson model is claimed to fit rheological data better than general viscoplastic models for many materials and is the preferred rheological model for blood and chocolate (1959).Dash *et al*. (1996) examined Casson fluid flow in a pipe with a homogeneous porous medium. Unsteady boundary layer flow of a Casson fluid due to an impulsively started moving with flat plate has been discussed by Mustafa *et al*. (2011). Eldabe and Salwa (1995) studied the flow and heat transfer of a Casson fluid between two rotating cylinder. Boyd *et al*. (2007) analyzed the Casson and Carreau-Yasuda non-Newtonian blood models in steady flow and oscillatory flow using Lattice Boltmann method. Recently Bhattacharyya *et al*. (2014) obtained the exact solution for boundary layer flow of Casson fluid over a permeable stretching/shrinking sheet. Mukhopadhyay (2013) studied the Casson fluid flow and heat transfer over a nonlinear stretching sheet. At the current investigation, we refer some latest studies on stretched flows. Rashidi and Mohimanian Pour (2010) obtained the analytic solutions for unsteady boundary-layer flow and heat transfer due to a stretching sheet by means of homotopy analysis method. Further Rashidi and Keimanesh (2010) use the differential transform method and Padé approximant for solving MHD flow in a laminar liquid film from a horizontal stretching surface. Rana and Bhargava (2012) studied the flow and heat transfer of a nanofluid over a nonlinearly stretching sheet. Radiation effect on a steady two-dimensional boundary layer flow of a dusty fluid over a stretching sheet is analyzed by Ramesh and Gireesha (2013).

Flow near stagnation-point is very interesting in fluid dynamics. Actually, the stagnation flow takes place whenever the flow impinges to any solid object and the local velocity of the fluid at the stagnation-point is zero. It is an important bearing on several industrial and technical applications such as cooling of electronic devices by fans, cooling of nuclear reactors during emergency shutdown, heat exchangers placed in a low-velocity environment, solar central receivers exposed to wind currents, and many hydrodynamic processes. The two-dimensional flow of a fluid near a stagnation point was first examined by Hiemenz (1911). Later Chiam (1994) analyzed steady two dimensional stagnation-point flow of an incompressible viscous fluid towards a stretching surface. Mahapatra and Gupta (2002) studied the stagnation-point flow towards a stretching sheet taking different stretching and straining velocities. Various important aspects of the stagnation-point flow over stretching sheet under were presented by many investigators (Nazar *et al*. 2004, Pal. 2009, Pop *et al*. 2011, Ramesh *et al* 2012, Ramesh *et al*.2014). Mustafa *et al*. (2012) obtained the analytical solution for stagnation-point flow and heat transfer of a Casson fluid towards a stretching sheet using HAM method. Later Hayat *et al*. (2013) investigated the mixed convection stagnation-point flow of an incompressible Casson fluid over a stretching sheet under convective boundary conditions. Further Nandy (2013) studied the hydromagnetic boundary layer flow and heat transfer of a non-Newtonian Casson fluid in the neighborhood of a stagnation point over a stretching surface in the presence of velocity and thermal slips. Two-dimensional magnetohydrodynamic stagnation-point flow of electrically conducting non-Newtonian Casson fluid and heat transfer towards a stretching sheet with thermal radiation have been reported by Bhattacharyya (2013). Parand *et al* (2012) studied the laminar boundary layer flow using numerical method. Akbar *et al*. (2013) obtained the Numerical solutions of Magnetohydrodynamic boundary layer flow of tangent hyperbolic fluid towards a stretching sheet via RKF45 method.

Aforementioned studies the boundary layer flow and heat transfer analysis is investigated for only flat stretching sheet. Study of flow and heat transfer of viscous fluids over stretching sheet with a variable thickness (non-flatness) can be more relevant to the situation in practical applications. For the first time Fang *et al*. (2012) obtain an elegant analytical and numerical solution to the two-dimensional boundary layer flow due to a non-flatness stretching sheet. Further this problem was extended by Subhashini *et al*. (2013) by including the energy equation and found that thermal boundary layer thicknesses for the first solution were thinner than those of the second solution. Numerical solution for the flow of a Newtonian fluid over a stretching sheet with a power law surface velocity, slip velocity and variable thickness was studied by Khaddar *et al*. (2013).

The present work is undertaken to study the effect of variable thickness on the boundary layer stagnation-point flow of Casson fluid over a stretching sheet. The thermal radiation effect in such configuration is also studied. Dimensionless expressions of velocity and temperature are solved numerically. The presented plots illustrate the behavior of pertinent parameters on the velocity and temperature. Numerical values of skin friction

coefficient and local Nusselt number are tabulated and analyzed. The results have possible technological applications in liquid-based systems involving stretchable materials.

2. PROBLEM FORMULATION

We consider the steady incompressible flow of Casson fluid over a stretching sheet located at $y = A(x+b)^{\frac{1-m}{2}}$ with a fixed stagnation point at $x = 0$ (figure 1). We assume that wall is impermeable, non-flat with a given profile and the coefficient A being small so that the sheet is sufficiently thin. Assume that the stretching sheet has a velocity $U(x) = U_0(x+b)^m$, where m is the velocity power index.

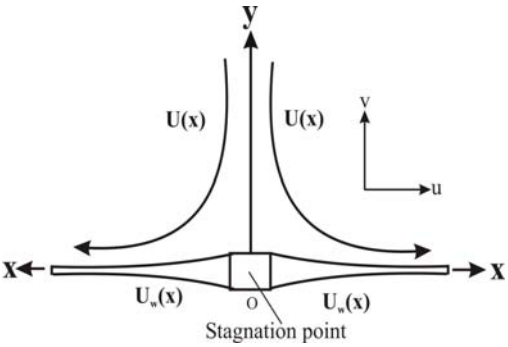

Fig. 1. Physical description of the considered problem.

The rheological equation of state for an isotropic and incompressible flow of a Casson fluid is

$$\tau_{ij} = 2\left(\mu_B + p_y/\sqrt{2\pi}\right)e_{ij}, \pi > \pi_c,$$
$$2\left(\mu_B + p_y/\sqrt{2\pi_c}\right)e_{ij}, \pi < \pi_c.$$

In above equation π is the product of the component of deformation rate with itself, i.e., $\pi = e_{ij}e_{ij}$ and e_{ij} is the $(i,j)^{th}$ component of the deformation rate, π_c is a critical value of this product based on the non-Newtonian model, μ_B is plastic dynamic viscosity of the non- Newtonian fluid, and p_y is the yield stress of the fluid.

The simplified two dimensional equations governing the flow in the boundary layer of a steady, laminar, and incompressible Casson fluid are (Bhattacharyya *et al*. 2014)

$$\frac{\partial u}{\partial x} + \frac{\partial v}{\partial y} = 0, \tag{1}$$

$$u\frac{\partial u}{\partial x} + v\frac{\partial u}{\partial y} = \nu\left(1+\frac{1}{\beta}\right)\frac{\partial^2 u}{\partial y^2} - \frac{1}{\rho}\frac{\partial p}{\partial x}, \tag{2}$$

$$\rho c_p\left(u\frac{\partial T}{\partial x} + v\frac{\partial T}{\partial y}\right) = k\frac{\partial^2 T}{\partial y^2} - \frac{\partial q_r}{\partial y}, \tag{3}$$

where u and v are the velocity components of the fluid along x and y directions, respectively, x is distance along the sheet, y is distance perpendicular to the sheet, μ, ρ, k and c_p are the co-efficient of viscosity of the fluid, density of the fluid, thermal conductivity and specific heat of the fluid respectively. $\beta = \mu_B\sqrt{2\pi_c}/p_y$ is Casson fluid parameter.

The associated boundary conditions for the present problem are [Fang *et al*. (2012)]

$$u = U_w(x), v = 0, T = T_w(x) = T_\infty + T_0(x+b)^{\frac{m}{2}}, \text{ at } y = A(x+b)^{\frac{1-m}{2}}, \tag{4}$$
$$u \to U(x),\ T \to T_\infty \text{ as } y \to \infty,$$

Where $U_w(x) = U_0(x+b)^m$ is the stretching velocity, U_0 and b is uniform velocity of sheet (i.e for $m = 0$) and b is a constant. T_w and T_∞ denote the temperature at the wall and at large distance from the wall respectively and T_0 is the characteristic temperature

By employing the generalized Bernoulli's equation, in free stream $U(x) = U_1(x+b)^m$, equation (2) becomes

$$U\frac{dU}{dx} = -\frac{1}{\rho}\frac{dp}{dx} \tag{5}$$

Using (5) into (2) one can obtain

$$u\frac{\partial u}{\partial x} + v\frac{\partial u}{\partial y} = \nu\left(1+\frac{1}{\beta}\right)\frac{\partial^2 u}{\partial y^2} + U\frac{dU}{dx} \tag{6}$$

Using the Rosseland approximation for radiation [19], radiation heat flux is simplified as

$$q_r = -\frac{4\sigma^*}{3k^*}\frac{\partial T^4}{\partial y}, \tag{7}$$

Where σ^* and k^* are the Stefan-Boltzman constant and mean absorption co-efficient, respectively. Assuming that the temperature differences within the flow such

that the term T^4 may be expressed as a linear function of the temperature, we expand T^4 in a Taylor series

about T_∞ and neglecting the higher order terms beyond the first degree in $(T - T_\infty)$ we get

$$T^4 \cong 4T_\infty^3 T - 3T_\infty^4. \tag{8}$$

Using (7) and (8), (3) reduces to

$$\rho c_p\left(u\frac{\partial T}{\partial x} + v\frac{\partial T}{\partial y}\right) = k\frac{\partial^2 T}{\partial y^2} - \frac{16\sigma^* T_\infty^3}{3k^*}\frac{\partial^2 T}{\partial y^2}. \tag{9}$$

The momentum and energy equations can be transformed using the following similarity transformation

$$\eta = \sqrt{\frac{(m+1)U_0}{2\nu}}\left[y(x+b)^{\frac{m-1}{2}} - A \right],$$

$$f = \frac{\psi}{\sqrt{\frac{2\nu U_0}{m+1}(x+b)^{m+1}}} \text{ and } \theta = \frac{T-T_w}{T_w - T_\infty}, \qquad (10)$$

where η is the similarity variable and ψ is the stream function defined as $u = \frac{\partial \psi}{\partial y}$ and $v = -\frac{\partial \psi}{\partial x}$, which identically satisfies equation (1). Substituting (10) into equations (6) and (9), we obtain the following ordinary differential equations:

$$\left(1+\frac{1}{\beta}\right) f'''(\eta) + f(\eta) f''(\eta) + \frac{2m}{m+1}\left[\lambda^2 - f'^2(\eta)\right] = 0 \qquad (11)$$

$$\left(1+\frac{4}{3}Nr\right)\frac{1}{\Pr}\theta''(\eta) + f(\eta)\theta'(\eta) - \frac{m}{m+1} f'(\eta)\theta(\eta) = 0 \qquad (12)$$

Subjected to the boundary conditions (4) which becomes

$$f(\eta) = \alpha\left(\frac{1-m}{1+m}\right),\ f'(\eta) = 1, \theta(\eta) = 1 \ at\ \eta = 0$$

$$f'(\eta) \to \lambda, \theta(\eta) \to 0 \text{ as } \eta \to \infty \qquad (13)$$

In the above equations, prime denote differentiation with respect to η and $\alpha = A\sqrt{\frac{U_0(m+1)}{2\nu}}$ is the wall thickness parameter, m is the velocity power index, $\lambda = \frac{U_1}{U_0}$ is the velocity ratio, $Nr = \frac{4\sigma^* T_\infty^3}{kk^*}$ is the radiation parameter and $\Pr = \frac{\mu c_p}{k}$ is the Prandtl number.

3. INTRODUCTION OF RUNGE-KUTTA-FEHLBERG METHOD

Runge-Kutta-Fehlberg method has a procedure to determine if the proper step size h is being used. At each step, two different approximations for the solution are made and compared. If the two answers are in close agreement, the approximation is accepted. If the two answers do not agree to a specified accuracy, the step size is reduced. If the answers agree to more significant digits than required, the step size is increased.

Step requires the following values

$$k_1 = hf(x_i, y_i)$$

$$k_2 = hf\left(x_i + \frac{1}{4}h, y_i + \frac{1}{4}k_1\right)$$

$$k_3 = hf\left(x_i + \frac{3}{8}h, y_i + \frac{3}{32}k_1 + \frac{9}{32}k_2\right)$$

$$k_4 = hf\left(x_i + \frac{12}{13}h, y_i + \frac{1932}{2197}k_1 - \frac{7200}{2197}k_2 + \frac{7296}{2197}k_3\right)$$

$$k_5 = hf\left(x_i + h, y_i + \frac{439}{216}k_1 - 8k_2 + \frac{3680}{513}k_3 - \frac{845}{4104}k_4\right)$$

$$k_6 = hf\left(x_i + \frac{1}{2}h, y_i - \frac{8}{27}k_1 + 2k_2 - \frac{3544}{2565}k_3 - \frac{1859}{4104}k_4 - \frac{11}{40}k_5\right)$$

An approximation to the solution is made using a Runge-Kutta method of order 4:

$$y_{i+1} = y_i + \frac{25}{216}k_1 + \frac{1408}{2565}k_3 + \frac{2197}{4104}k_4 - \frac{1}{5}k_5$$

A better value for the solution is determined using Runge-Kutta method of order 5:

$$z_{i+1} = y_i + \frac{16}{135}k_1 + \frac{6656}{12{,}825}k_3 + \frac{28{,}561}{56{,}430}k_4 - \frac{9}{50}k_5 + \frac{2}{55}k_6$$

4. NUMERICAL SOLUTION

The non-linear coupled equations (11) and (12) along with boundary conditions (13) are solved numerically using Runge-Kutta-Fehlberg method with a shooting technique. In the shooting method, it is essential to select a suitable finite value of $\eta \to \infty$. The step size $\Delta\eta = 0.001$ issued to obtain the numerical solution with η_∞. The asymptotic converged results within a tolerance level of 10^{-6} are obtained. Table 1 represents a comparison of $f''(0)$ obtained in the present work and those work obtained earlier by Fang *et al*. (2012) in the absence of $\lambda, \alpha, \Pr, Nr$ and β. It is clearly observed that good agreement between the results exists. This lends confidence in the numerical method. It is also observed from Table 2, that the numerical values of $\theta'(0)$ in the present paper for different value of $\Pr, m$ are in good agreement with results obtained by Rana and Bhargava (2012) and Zaimi *et al*. (2014)

5. GRAPHICAL RESULTS AND DISCUSSION

We discuss the influences of different parameters $\alpha, \beta, \lambda, m, Nr$ and $\Pr$ on velocity and temperature fields. Figures 2 and 3, respectively

represents the velocity and temperature profiles for various values of velocity ratio parameter λ. In figure 2, we can see that two different classes (types) of boundary layers. In the first class, the velocity of fluid inside the boundary layer decreases from the surface towards the edge of the layer ($\lambda<1$) and in the second type the fluid velocity increases from the surface towards the edge ($\lambda>1$). One important note that if $\lambda=1$, the stretching velocity and the straining velocity are equal, then there is no boundary layer of Casson fluid flow near the sheet, this is similar to that of Chiam's (1994) observation for Newtonian fluid. In Fig. 3, one can see that in all cases thermal boundary layers formed and the temperature at a point decreases with increase of λ.

Table 1 Comparison of the values of skin friction coefficient $f''(0)$ for various values of m in the case of $\lambda=\alpha=\Pr=Nr=0$ and $\beta=0.5$

m	Fang *et al*. (2012)	Present result
10.0	-1.0603	-1.06034
9.0	-1.0589	-1.05893
7.0	-1.0550	-1.05506
5.0	-1.0486	-1.04862
3.0	-1.0359	-1.03588
2.0	-1.0234	-1.02342
1.0	-1.0000	-1.00000
0.5	-0.9799	-0.97994
0.0	-0.9576	-0.95764

Table 2 Comparison of the values of $\left|-\theta'(0)\right|$ for various values of m in the case of $\lambda=\alpha=\beta=Nr=N_b=N_t=0$

Pr	m	Rana and Bhargava (2012)	Zaimi et. al (2014)	Present result
1	0.2	0.6113	0.61131	0.611310
	0.5	0.5967	0.5668	0.596687
	1.5	0.5768	0.57686	0.576869
	2.0	---	0.57245	0.5724553
	3.0	0.5672	0.56719	0.5724553
	4.0	---	0.56415	0.5641562
	8.0	---	0.55897	0.5589740
	10.0	0.5578	0.55783	0.5578319
5	0.1	---	1.61805	1.6180573
	0.2	1.591	1.60757	1.6075742
	0.3	---	1.59919	1.5991913
	0.5	1.5839	1.58658	1.5865846
	0.8	---	1.57E+00	1.5738902
	1.0	---	1.57E+00	1.5678702
	1.5	1.5496	1.55751	1.5575188
	2.0	---	1.55093	1.5509317
	2.5	---	1.54636	1.5463670
	3.0	1.5372	1.54271	1.5430156
	10.0	1.526	1.52877	1.5287732

Figures 4 and 5 illustrate the influence of the Casson fluid parameter β on the velocity and temperature profiles respectively. One note that the velocity increases with the increase in values of β for λ ($\lambda>1$) and it decreases with β for λ ($\lambda<1$). Consequently, the velocity boundary layer thickness reduces for both values of λ .The effect of Casson parameter on the temperature profiles is depicted in figure 5 and noticed that at a point temperature increases with increasing of β.

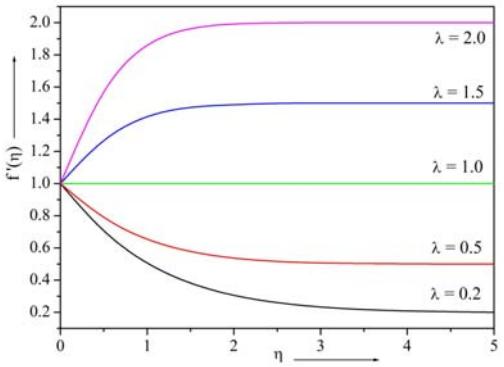

Fig. 2. Velocity profile for λ with $\alpha=0.5,\beta=2,m=2,\Pr=3,Nr=2$.

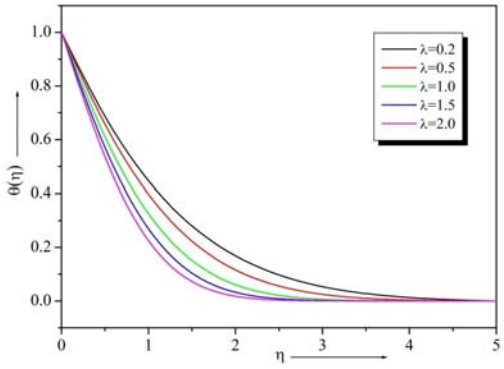

Fig. 3. Temperature profile for λ with $\alpha=0.5,\beta=2,m=2,\Pr=3,Nr=2$.

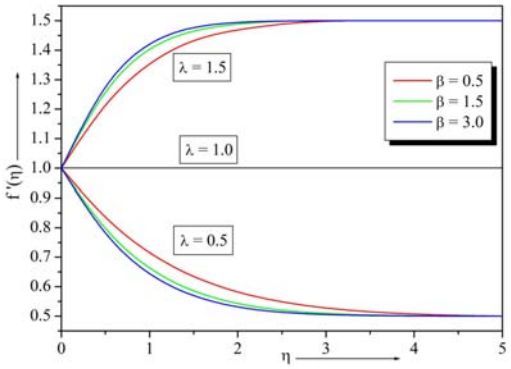

Fig. 4. Velocity profile for β with $\alpha=0.5,m=2,\Pr=3,Nr=2$.

Figure 6 exhibits the variation in the velocity profiles for different values of α .This figure indicates that if α increases the fluid velocity $f'(\eta)$ is increases for a fixed value of $\lambda<1$. On the other hand when $\lambda>1$, the fluid velocity decreases with the increase of α. This is because for higher value of α the boundary layer

becomes thicker. The temperature profile for different values of α for a fixed value of λ is plotted in figure 7. As it can be noticed, an increase in the wall thickness parameter results in an increase of the temperature of fluid.

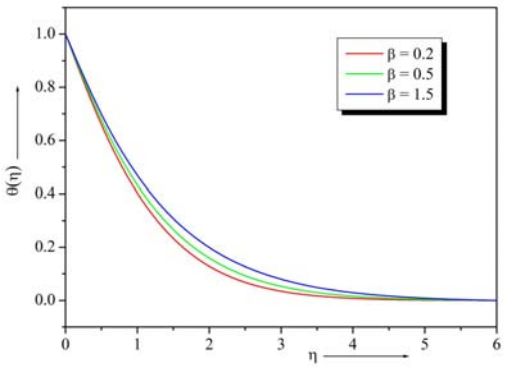

Fig. 5. Temperature profile for β with $\alpha = 0.5, \lambda = 1.5, m = 2, \Pr = 3, Nr = 2$ **.**

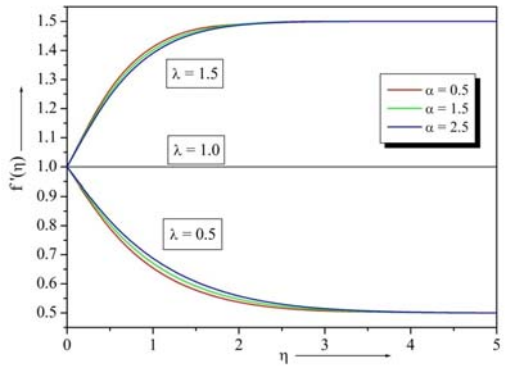

Fig. 6. Velocity profile for α with $\beta = 2, m = 2, \Pr = 3, Nr = 2$ **.**

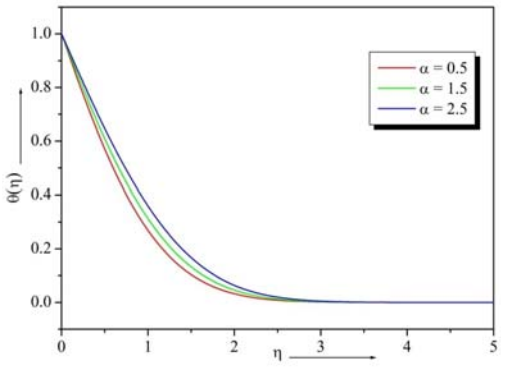

Fig. 7. Temperature profile for α with $\beta = 2, \lambda = 1.5, m = 2, \Pr = 3, Nr = 2$ **.**

Figure 8 shows the effect of on the velocity profiles for the fixed values of other parameters. One can clearly observed that velocity increases with the decrease of and reverse effect can be found when. This indicates that the momentum boundary thickness becomes thinner as increases along the sheet. For a constant valued of temperature increases with the increase of as shown in figure 9. From equation (13), one knows that if the problem reduces to flat sheet problem.

Figure 10 depicts the effect of Prandtl number Pr on temperature distributions for a fixed value of λ. An increase in Prandtl number reduces the thermal boundary layer thickness. Prandtl number signifies the ratio of momentum diffusivity to thermal diffusivity. Fluids with lower Prandtl number will possess higher thermal conductivities so that heat can diffuse from the wall faster than for higher Pr fluids. Hence Prandtl number can be used to increase the rate of cooling in conducting flows. From figure 11, it is observed that an increase the value of thermal radiation parameter Nr produces a significant increase in the thickness of the thermal boundary layer, so the temperature distribution increases with increasing the value of Nr.

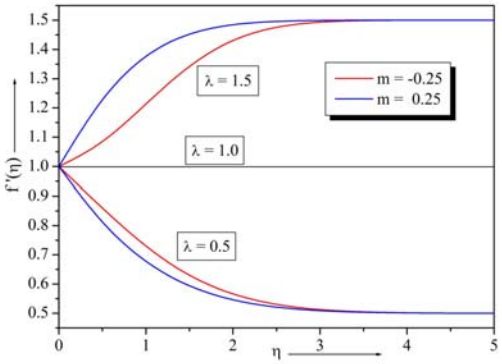

Fig. 8. Velocity profile for m with $\beta = 2, \alpha = 0.5, \Pr = 3, Nr = 2$ **.**

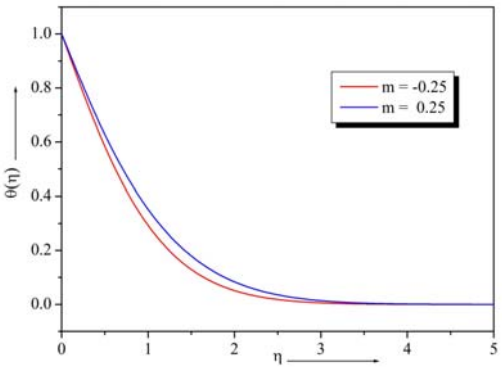

Fig. 9. Temperature profile for m with $\beta = 2, \lambda = 1.5, \alpha = 0.5, \Pr = 3, Nr = 2$ **.**

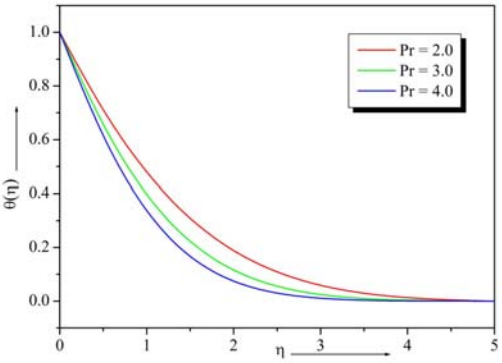

Fig. 10. Temperature profile for Pr **with** $\beta = 2, \alpha = 0.5, m = 2, Nr = 2$ **.**

Table 3 Skin friction coefficient $-f''(0)$ and Nusselt number $-\theta'(0)$ for different values of $\alpha, \Pr, Nr, m$ and β

α	Pr	Nr	m	β	$\lambda = 0.5$		$\lambda = 1.5$	
					$-f''(0)$	$-\theta'(0)$	$f''(0)$	$-\theta'(0)$
0.5	3	2	2	3	0.612784	0.820352	0.852615	1.040076
1.0					0.582278	0.749220	0.820171	0.964867
1.5					0.553279	0.683084	0.788808	0.893380
0.5	2	2	2	3	0.612784	0.668615	0.852615	0.869990
	3				0.612784	0.820352	0.852615	1.040076
	4				0.612784	0.946463	0.852615	1.178240
0.5	3	1	2	3	0.612784	1.025809	0.852615	1.264194
		2			0.612784	0.820352	0.852615	1.040076
		3			0.612784	0.701657	0.852615	0.907529
0.5	3	2	-0.25	3	0.287866	1.013823	0.062329	1.082265
			0		0.437557	0.929517	0.504290	1.063871
			0.25		0.501850	0.888662	0.640387	1.054115
0.5	3	2	2	0.5	0.415718	0.849439	0.575779	1.018303
				1.5	0.551059	0.828760	0.765721	1.033967
				3	0.612784	0.820352	0.852615	1.040076

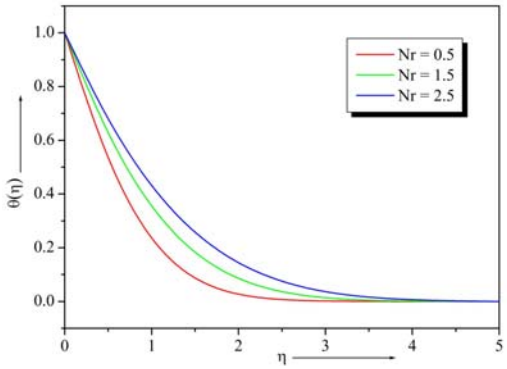

Fig. 11. Temperature profile for Nr with $\beta = 2, \alpha = 0.5, m = 2, \Pr = 3$.

One can note down that momentum equation and heat transfer equation are mutually coupled and the skin friction and Nusselt number coefficient are very important in engineering applications. Therefore the values of $-f''(0)$ and $-\theta'(0)$ are presented in Table 3 for various values of governing parameters at $\lambda < 1$ and $\lambda > 1$. It can be seen from the table that the effect of increasing the values of α is to increase the skin friction, whereas m, β are decreases. Similarly the increasing values of α, Nr, m, β is to increase the Nusselt number but the opposite effect can be seen in $\Pr$. Also one can observe that there is no change in the skin friction when Pr and Nr varies.

6. CONCLUSIONS

The main results of present investigation can be listed below.

- Velocity boundary layer thickness decreases with increasing velocity ratio parameter.
- An increase in the Casson parameter decreases the velocity field and increases the temperature field.
- Larger values of wall thickness parameter increase the velocity and temperature boundary layer thicknesses.
- Velocity decreases and temperature increases with the increase of velocity power index.
- Increase of Prandtl number reduces the thermal boundary layer thickness.
- Temperature increases with increasing values of the radiation parameter. This phenomenon is approved to a higher effective thermal diffusivity.

ACKNOWLEDGEMENTS

The authors are thankful to the referee for his valuable suggestions. One of the author (B. C. Prasanna Kumara) gratefully acknowledges the financial support of University Grants Commission (UGC F. NO. 43-419/2014 (SR)), Delhi, India for pursuing this work.

REFERENCES

Akbar, N. S., S. Nadeem, R. U. Haq and Z. H. Khan (2013). Numerical solutions of Magnetohydrodynamic boundary layer flow of tangent hyperbolic fluid towards a stretching sheet. *Indian J. Phys.* 87(11), 1121–1124.

Bhattacharyya, K. (2013). MHD stagnation-point flow of Casson fluid and heat transfer over a stretching sheet with thermal radiation. *J. Thermodynamics* 9.

Bhattacharyya, K., T. Hayat and A. Alsaedi (2014). Exact solution for boundary layer flow of Casson fluid over a permeable stretching/shrinking sheet. *Z. Angew. Math. Mech.* 94(6)522–528.

Boyd, J., J. M. Buick and S. Green (2007). Analysis of the Casson and Carreau- Yasuda non-Newtonian blood models in steady and

oscillatory flow using the lattice Boltzmann method. *Phys. Fluids*. 93-103.

Casson, N. (1959). *Rheology of dispersed system, Oxford: Pergamon Press* 84.

Chiam, T. C. (1994). Stagnation-point flow towards a stretching plate. *J. Phys. Soc. Jpn.* 63, 2443–2444.

Dash, R. K., K. N. Mehta and G. Jayaraman (1996). Casson fluid flow in a pipe filled with a homogeneous porous medium. *Int. J. Eng. Sci.* 34(10) 1145-1156.

Eldabe, N. T. M. and M. G. E. Salwa (1995). Heat transfer of MHD non-Newtonian Casson fluid flow between two rotating cylinder. *J. Phys. Soc.Jpn.* 6441–64.

Fang, T., J. I. Zhang and Y. Zhong (2012). Boundary layer flow over a stretching sheet with variable thickness. *Applied Mathematics and Computation* 218, 7241–7252.

Hayat, T., S. A. Shehzad, A. Alsaedi and M. S. Alhothuali (2012). Mixed Convection Stagnation Point Flow of Casson Fluid with Convective Boundary Conditions. *Chin. Phys. Lett.* 29(11), 114704.

Hiemenz, K. (1911). Die grenzschicht an einem in dengleich formigen flussigkeitsstrom eingetauchten geraden kreiszlinder. *Dingl. Polytec. J.* 326, 321–328.

Khader, M. M. and A. M. Megahed (2013). Numerical solution for boundary layer flow due to a nonlinearly stretching sheet with variable thickness and slip velocity. *Eur. Phys. J. Plus* 128:100 10.1140/epjp/I 2013-13100-7.

Mahapatra, T. R. and A. S. Gupta (2002). Heat transfer in stagnation pint flow towards a stretching sheet. *Heat Mass Transf.* 38, 517–521.

Mukhopadhyay, S. (2013). Casson fluid flow and heat transfer over a nonlinearly stretching, *Chin. Phys.* 22(7), 074701.

Mustafa, M., T. Hayat, I. Pop and A. Aziz (2011). Unsteady boundary layer flow of a Casson fluid due to an impulsively started moving flat plate. *Heat Transfer-Asian Resc.* 40(6) 563-576.

Mustafa, M., T. Hayat, I. Pop and A. Hendi (2012). Stagnation-point flow and heat transfer of a Casson fluid towards a stretching sheet, Z Naturforsch. 67, 70-76.

Nandy, S. K. (2013). Analytical solution of MHD stagnation-point flow and heat transfer of Casson fluid over a stretching sheet with partial slip. *ISRN Thermodynamic*s 9.

Nazar, R., N. Amin, D. Filip and I. Pop (2004). Stagnation point flow of a micropolar fluid towards a stretching sheet. *Int. J. Nonlinear Mech.* 39, 1227–1235.

Pal, D. (2009). Heat and mass transfer in stagnation-point flow towards a stretching surface in the presence ofbuoyancy force and thermal radiation. *Meccanica* 4, 145–158.

Parand, K., M. Shahini and M. Dehghan (2010). Solution of a laminar boundary layer flow via numerical method. *Com. Non. Sci. Num. Sim*. 15(2), 360-367.

Pop, I., A. Ishak and F. Aman (2011). Radiation effects on the MHD flow near the stagnation point of a stretching sheet: revisited. *Z. Angew. Math. Phys.* 62(5), 953-956.

Ramesh, G. K. and B. J. Gireesha (2013). Flow over a stretching sheet in a dusty fluid with radiation effect. *J heat transfer* 135102702(1-6).

Ramesh, G. K., B. J. Gireesha and C. S. Bagewadi (2012). MHD flow of a dusty fluid near the stagnation point over a permeable stretching sheet with non-uniform source/sink. *Int. J.Heat and Mass Transf.* 55, 4900–4907.

Ramesh, G. K., B. J. Gireesha and C. S. Bagewadi (2014). Stagnation point flow of a MHD dusty fluid towards a stretching sheet with radiation. *Afr. Mat.* 25(1), 237-249.

Rana, P. and R. Bhargava (2012). Flow and heat transfer of a nanofluid over a nonlinearly stretching sheet: a numerical study. *Comm. Nonlinear Sci. Num. Simul.* 17, 212-226.

Rashidi, M. M. and M. Keimanesh (2010). Using differential transform method and Padé approximant for solving MHD flow in a laminar liquid film from a horizontal stretching surface. *Mathematical Problems in Engineering*,. Article ID 491319, 14.

Rashidi, M. M. and S. A. Mohimanian Pour (2010). Analytic approximate solutions for unsteady boundary-layer flow and heat transfer due to a stretching sheet by homotopy analysis method. *Nonlinear Analysis: Modelling and Control* 15(1), 83–95.

Subhashini, S. V., R. Sumathi and I. Pop (2013). Dual solutions in a thermal diffusive flow over a stretching sheet with variable thickness. *Int. Com. Heat and Mass Transf.* 48 61–66.

Zaimi, K., A. Ishak and I. Pop (2014). Boundary layer flow and heat transfer over a non linearly permeable stretching/shrinking sheet in a nanofluid. *Scientific Reports* 4, 4404(1-8).